

On the Application of Accelerated Molecular Dynamics to Liquid Water Simulations

César Augusto F de Oliveira,* Donald Hamelberg, and J. Andrew McCammon

Department of Chemistry and Biochemistry and Department of Pharmacology, Center for Theoretical Biological Physics, Howard Hughes Medical Institute, University of California at San Diego, La Jolla, California 92093

Received: May 9, 2006; In Final Form: August 10, 2006

Our group recently proposed a robust bias potential function that can be used in an efficient all-atom accelerated molecular dynamics (MD) approach to simulate the transition of high energy barriers without any advance knowledge of the potential-energy landscape. The main idea is to modify the potential-energy surface by adding a bias, or boost, potential in regions close to the local minima, such that all transitions rates are increased. By applying the accelerated MD simulation method to liquid water, we observed that this new simulation technique accelerates the molecular motion without losing its microscopic structure and equilibrium properties. Our results showed that the application of a small boost energy on the potential-energy surface significantly reduces the statistical inefficiency of the simulation while keeping all the other calculated properties unchanged. On the other hand, although aggressive acceleration of the dynamics simulation increases the self-diffusion coefficient of water molecules greatly and dramatically reduces the correlation time of the simulation, configurations representative of the true structure of liquid water are poorly sampled. Our results also showed the strength and robustness of this simulation technique, which confirm this approach as a very useful and promising tool to extend the time scale of the all-atom simulations of biological system with explicit solvent models. However, we should keep in mind that there is a compromise between the strength of the boost applied in the simulation and the reproduction of the ensemble average properties.

Introduction

Owing to its key role in environmental sciences, industrial technology, and virtually all biological processes, water is by far the most studied liquid by computer simulations.¹ Water plays different roles with respect to protein properties, enzyme–substrate binding, and catalysis.² Computer simulation of such systems often involves the application of either molecular dynamics (MD) or Monte Carlo (MC) techniques to sample the conformational space of a large number of atoms. Simulations with explicit water solvent incur a significant computational cost associated with the large number of solvent molecules. Although continuum dielectric models have been successfully applied in macromolecular simulations,^{3,4} for a complete understanding of the behavior of many biochemical systems, an explicit treatment of water is essential.^{5–7} Modeling solvent effects by an implicit representation of the solvent is computationally most efficient, but has been shown in some cases to stabilize conformers other than the native structure⁸ and to lead to less realistic behavior than an explicit treatment of the solvent.⁹ In addition, some proteins show highly structured and localized water molecules in their binding sites, which play important roles in the protein–ligand interactions.^{10,11} In this case, a description in which all atomic and structural details of the solvent molecules are ignored may result in deleterious effects in simulations of protein function. Therefore, there is a need for the development of methods that make feasible the atomistic computer simulation of biological systems over long time scales. In other words, it is of great interest to extend the time scale accessible to all-atom explicit solvent molecular dynamics simulations in order to capture the long-time behavior of the biomolecules.

To address this question, a very promising simulation method for biomolecules was recently proposed by Hamelberg et al.¹² This approach, based on an earlier work of Voter,^{13,14} consists of an all-atom molecular dynamics technique that can accelerate the simulations without advance knowledge of the potential-energy wells or barriers. The main idea is to modify the potential-energy surface by adding a bias potential in regions close to the local minima, such that all transitions rates are increased. Unlike Voter's implementation, this method does not require diagonalization of the Hessian matrix at each simulation step to identify the transition state regions, and hence it can be applied to a much larger systems. Previous results showed that the accelerated molecular dynamics method proposed by our group¹² indeed simulated the barrier crossing transition with ease and, as a result, enhanced conformational sampling as compared to regular MD.¹⁵ Although in that work an implicit representation was used to describe the solvent environment, it is of interest to consider explicit solvation.

In the present work we show the first results of the application of accelerated MD simulation method to liquid water. Here we investigated the effect of the bias potential on its dynamics, structure and ensemble-average properties. Our results, in agreement with Hamelberg's previous work, show the strength and robustness of this simulation technique, which confirm this approach as a very useful and promising tool to extend the time scale of the all-atom simulations of biological systems with explicit solvent models.

Methods

In this section, we give a brief description of the accelerated MD method. More details are found in ref 12. The basic ideas behind the accelerated molecular dynamic method consist in

* To whom correspondence should be addressed. E-mail: cesar@mccammon.ucsd.edu.

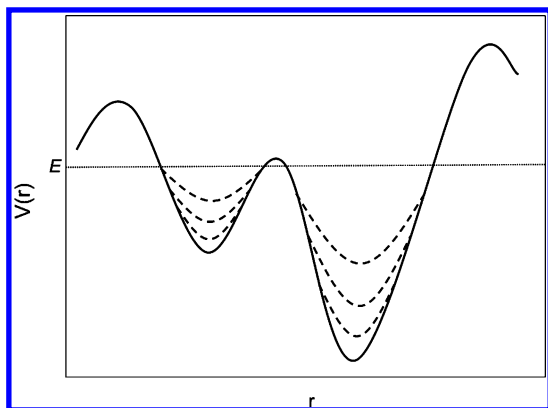


Figure 1. Schematic representation of a hypothetical true (solid line) and modified (dashed line) potential-energy function with different values of α . The modified potential converges to the true potential at large values of α . The dotted line corresponds to the boost energy E .

the construction of a new potential-energy surface $V^*(r)$ by applying a bias boost potential, $\Delta V(r)$, to the true potential $V(r)$. The bias potential is a nonnegative continuous function of the atomic coordinates r that modifies the potential surface whenever the unmodified (true) potential is below a predefined value E , the boost energy. Equation 1 shows the relation among the unmodified, modified, and boost energy.

$$V^*(r) = \begin{cases} V(r), & V(r) \geq E \\ V(r) + \Delta V(r), & V(r) < E \end{cases} \quad (1)$$

In this work, $\Delta V(r)$ is defined by eq 2, according to the implementation proposed by Hamelberg et al.¹²

$$\Delta V(r) = \frac{(E - V(r))^2}{\alpha + (E - V(r))} \quad (2)$$

where α is a tuning parameter that controls the depth of the energy basins on the modified potential. Figure 1 illustrates the effect of the eq 2 on a hypothetical one-dimensional potential function $V(r)$. The dashed lines represent the effect of variation of the parameter α on the modified potential surface. It is worth noting that the modified potential surface reflects the underlying shape of the true potential and increases the escape rate of the system from local minima regions by lowering the barriers of the potential-energy landscape. As previously described,^{12,15} E and α control the extent to which MD will be accelerated. In addition to determining how deep the energy basins are on the modified potential, the parameter α also modifies the local roughness of the potential-energy landscape. Keeping E constant, the α parameter smoothes or roughens the potential surface when its value is decreased or increased, respectively.¹⁵ The only restriction about the chosen value for E is that it should be greater than the minimum of $V(r)$, $V_{\min}(r)$. This condition ensures that the MD simulation will be accelerated to some degree. The regular MD simulation can be restored by simply setting a value for E less than $V_{\min}(r)$.

The accelerated MD method also permits one to recover the correct canonical averages of an observable $A(r)$ calculated from configurations sampled on the modified potential-energy surface. The canonical ensemble average of an observable $A(r)$ is given by

$$\langle A \rangle = \frac{\int dr A(r) \rho(r)}{\int dr \rho(r)} \quad (3)$$

where $\rho(r)$ is the canonical distribution function,

$$\rho(r) = \exp(-\beta V(r)) \quad (4)$$

and $\beta = 1/kT$, T is the temperature, and k is the Boltzmann's constant. In the case where a non-Boltzmann sampling is employed, eq 3 can be rewritten as

$$\langle A \rangle = \frac{\int dr A(r) \rho^*(r) [\rho(r)/\rho^*(r)]}{\int dr \rho^*(r) [\rho(r)/\rho^*(r)]} \quad (5)$$

where $\rho^*(r)$ corresponds to a non-Boltzmann distribution function. In the accelerated MD method, we can define $\rho^*(r)$ as a Boltzmann distribution function in the same temperature, but corresponding to the modified potential $V^*(r)$. Thus,

$$\frac{\rho(r)}{\rho^*(r)} = \frac{\exp(-\beta V(r))}{\exp(-\beta V^*(r))} = \frac{\exp(-\beta V(r))}{\exp(-\beta [V(r) + \Delta V(r)])} = \exp(\beta \Delta V(r)) \quad (6)$$

which corresponds to the Boltzmann factor of the bias energy. Substituting eq 6 into eq 5, we get

$$\langle A \rangle = \frac{\int dr A(r) \exp(-\beta V(r) - \beta \Delta V(r)) \exp(\beta \Delta V(r))}{\int dr \exp(-\beta V(r) - \beta \Delta V(r)) \exp(\beta \Delta V(r))} = \frac{\int dr A(r) \exp(-\beta V(r))}{\int dr \exp(-\beta V(r))} \quad (7)$$

Therefore, correct canonical ensemble averages on the unmodified potential $V(r)$ can be obtained in the accelerated MD simulation by reweighting each configuration sampled on the modified potential $V^*(r)$ by the factor $\exp(\beta \Delta V(r))$. This procedure guarantees that the ensemble average obtained as time average over the trajectory generated from the modified potential is Boltzmann weighted.¹⁶

The simulations were carried out using TIP3P water molecules, which correspond to the most commonly used water model today.¹⁷ In this model the interaction sites are centered on the nuclei. Each site has a partial charge for computing the intermolecular Coulomb energy, and the only additional energy term is a Lennard-Jones interaction between oxygen atoms.

$$V(r) = \sum_i \sum_j \frac{q_i q_j \epsilon^2}{r_{ij}} + 4\epsilon \left[\left(\frac{\sigma}{r_{oo}} \right)^{12} - \left(\frac{\sigma}{r_{oo}} \right)^6 \right] \quad (8)$$

Since both electrostatic and van der Waals interactions play crucial roles in the liquid water simulations, in this work, the accelerated MD method was applied to the whole potential (equation 8).

The Leap module of the AMBER package was used to build the starting configuration of our liquid water model. The system consisted of 1126 TIP3P water molecules within a cubic box with edges of 36 Å. This initial configuration was relaxed by applying 100 steps of a steepest descent algorithm followed by 900 steps of conjugate gradient algorithm. The final configuration was then used as starting point for the subsequent MD simulations. First, to bring the system to its correct density, we carried out an MD simulation for 100 ps in which the NPT ensemble ($T = 300$ K, $P = 1$ atm) was applied. To further relax the system, we performed an additional MD simulation for 500 ps in which the NVT ensemble ($T = 300$ K, $\rho = 0.980$ g/mL)

TABLE 1: Heat of Vaporization ΔH_{vap} , Self-Diffusion Coefficient D , and Correlation Time τ Calculated from the Normal and Accelerated Molecular Dynamics Simulations^{a,b}

		ΔH_{vap}	$D_{\text{ACC}}/D_{\text{MD}}$	$\tau_{\text{MD}}/\tau_{\text{ACC}}$
normal MD				
$E = -9.57$	$\alpha = 0.02$	10.13	1.00	1.0
$E = -9.56$	$\alpha = 0.03$	10.18	1.00	≈ 2.3
$E = -9.55$	$\alpha = 0.04$	10.12	1.00	≈ 2.5
$E = -9.15$	$\alpha = 0.44$	10.13	1.00	≈ 4.0
	$\alpha = 0.88$	9.82	1.35	≈ 40.0
$E = -8.70$	$\alpha = 0.89$	10.05	1.15	≈ 2.0
	$\alpha = 8.88$	9.46	1.73	
	$\alpha = 8.88$	9.88	1.32	≈ 2.8
	$\alpha = 44.40$	10.06	1.10	≈ 1.0
$E = -6.93$	$\alpha = 2.66$	8.40	2.57	
$E = -4.80$	$\alpha = 4.80$	7.65	2.93	
$E = -2.49$	$\alpha = 7.10$	7.18	3.07	

^a ΔH_{vap} , E , and α in kcal/mol. ^b MD and ACC stand for normal and accelerated molecular dynamics simulation, respectively.

was applied. Hereafter, unless otherwise stated, all the simulations were performed in the above NVT ensemble condition. All data collection was carried out over MD simulations of 2 ns. To understand the role of the parameters of α and E in the simulation of liquid water, different schemes were applied in the accelerated MD simulations, which will be discussed in detail below.

As previously suggested,¹² we started setting α to a value close to $E - V_{\text{min}}$. Since large molecules and liquids tend to have multiple minima very close together, we suggest calculating an average potential energy, $\langle V(r) \rangle$, on the true potential over a short period of time and using that as the minimum, V_{min} . Thus, to estimate V_{min} , we calculated $\langle V(r) \rangle$ over five MD simulations of 20 ps starting from the same initial structure. The final value of -9.59 kcal/mol (potential energy/numbers of molecules) for V_{min} was obtained by averaging out the five values of $\langle V(r) \rangle$. The values of E and α applied in the accelerated MD simulations are presented in Table 1.

All calculations were performed using the Sander module in the AMBER7 package¹⁸ that was modified to carry out the accelerated molecular dynamics simulation. The equations of motion were integrated every 2.0 fs using the Verlet Leapfrog algorithm.¹⁹ For further analysis, the trajectory was sampled every 0.2 ps. During the MD runs, temperature and pressure were controlled via a weak coupling to external temperature and pressure baths with coupling constants of 0.5 and 1.0 ps, respectively.²⁰ The center-of-mass motion was removed at regular intervals of 10 ps. The PME summation method^{21,22} was used to treat the long-range electrostatic interactions in the minimization and simulation steps. The short-range nonbonded interactions were truncated using a 13 Å cutoff, and the nonbonded pair list was updated every 10 steps.

Results and Discussion

To explore the influence of the parameters E and α on the simulation results for liquid water, we applied eight different variations of the accelerated MD method and monitored the effects on the calculated self-diffusion coefficient (D), radial distribution function (RDF), heat of vaporization (ΔH_{vap}) and correlation time (τ) in the simulations. The heat of vaporization, ΔH_{vap} , when all degrees of freedom are treated classically, is calculated using the following equation:¹

$$\Delta H_{\text{vap}} = (\langle E_{\text{g}}^{\text{intra}} \rangle - \langle E_{\text{l}}^{\text{intra}} \rangle) + \frac{\langle E_{\text{g}}^{\text{inter}} \rangle - \langle E_{\text{l}}^{\text{inter}} \rangle}{N} + RT \quad (9)$$

where $\langle \rangle$ corresponds to an ensemble average, $E_{\text{g}}^{\text{intra}} - E_{\text{l}}^{\text{intra}}$ is

the difference in the intramolecular component of the internal energy of a water molecule in the two phases, and $E_{\text{g}}^{\text{inter}} - E_{\text{l}}^{\text{inter}}$ is the variation in the intermolecular component of the internal energy associated with the vaporization process. $\langle E^{\text{intra}} \rangle = 0$ in both phases as a result of the internal constraint applied to each TIP3P water molecule. N is the number of molecules in the cubic box used in the simulations. Assuming ideal gas behavior, the term RT , where R is the gas constant and T is the absolute temperature, equals the work of expansion $P\Delta V$ in a constant-pressure process. Thus, eq 9 can be rewritten as

$$\Delta H_{\text{vap}} = -\frac{\langle E_{\text{l}} \rangle}{N} + RT \quad (10)$$

The potential energy of the system was recorded every 100 steps for the calculation of heat of vaporization. $\langle E_{\text{l}} \rangle$ was obtained from the last 2 ns of the normal and accelerated MD simulations by reweighting each configuration by its respective Boltzmann factor of the bias potential, $\exp(\beta\Delta V(r))$.

By using the Einstein relation,²³ we calculated three-dimensional self-diffusion coefficients at 300 K for water molecules. This property, which is related to the mean-square displacement, $\langle |r_i(t + \Delta t) - r_i(t)|^2 \rangle$, is given by

$$6D\Delta t = \lim_{\Delta t \rightarrow \infty} \langle |r_i(t + \Delta t) - r_i(t)|^2 \rangle \quad (11)$$

where D is the center of mass self-diffusion coefficient, $r_i(t)$ are the molecular positions at time t , and Δt is the time interval between the initial position and the position at time t . To reduce the statistical error, the mean-square displacement was averaged over all molecules to obtain the self-diffusion coefficient for water in the bulk liquid. To further reduce the statistical error, the mean-square displacement was averaged over 20 blocks of 100 ps taken from the last 2 ns of the simulation. The diffusion coefficient obtained for each block was used to calculate the fluctuation around the mean value. Figure 2 plots the mean-square displacement versus Δt for water under normal and different accelerated MD conditions. The slopes of the plots are equal to $6D$. The oxygen–oxygen radial distribution functions (R_{oo}) were calculated over blocks of 20 ps taken from the last 2 ns of the trajectories. To smooth the RDFs' curves, the final oxygen–oxygen radial distribution functions were then obtained by averaging the R_{oo} obtained for each block. As shown before, to recover the correct canonical radial distribution functions, the R_{oo} calculated for each saved configuration on the modified potential was reweighted by its respective Boltzmann factor of the bias potential, $\exp(\beta\Delta V(r))$. Figure 3 shows the R_{oo} values obtained for the normal and all accelerated MD simulations.

As can be seen in Figure 2a, setting the boost energy, E , and α to -9.57 and 0.02 , -9.56 and 0.03 , and 9.55 and 0.04 kcal/mol, respectively, does not affect the calculated self-diffusion coefficient of the water molecules. In other words, the variation of mean-square displacement of the water molecules over time interval Δt calculated from the accelerated MD simulations was the same as the one obtained from normal MD. The diffusion coefficient obtained from the normal MD trajectory was $5.9 \pm 0.2 \times 10^{-5}$ cm²/s, in very good agreement with the value reported in the literature for TIP3P water simulations using Ewald summation.^{24,25} In addition, the R_{oo} values and ΔH_{vap} obtained from these accelerated MD schemes showed an excellent agreement with the ones calculated from the normal MD trajectory (Figure 3a and Table 1). On the other hand, by using E equal to -6.93 , -4.80 , and -2.49 kcal/mol, which

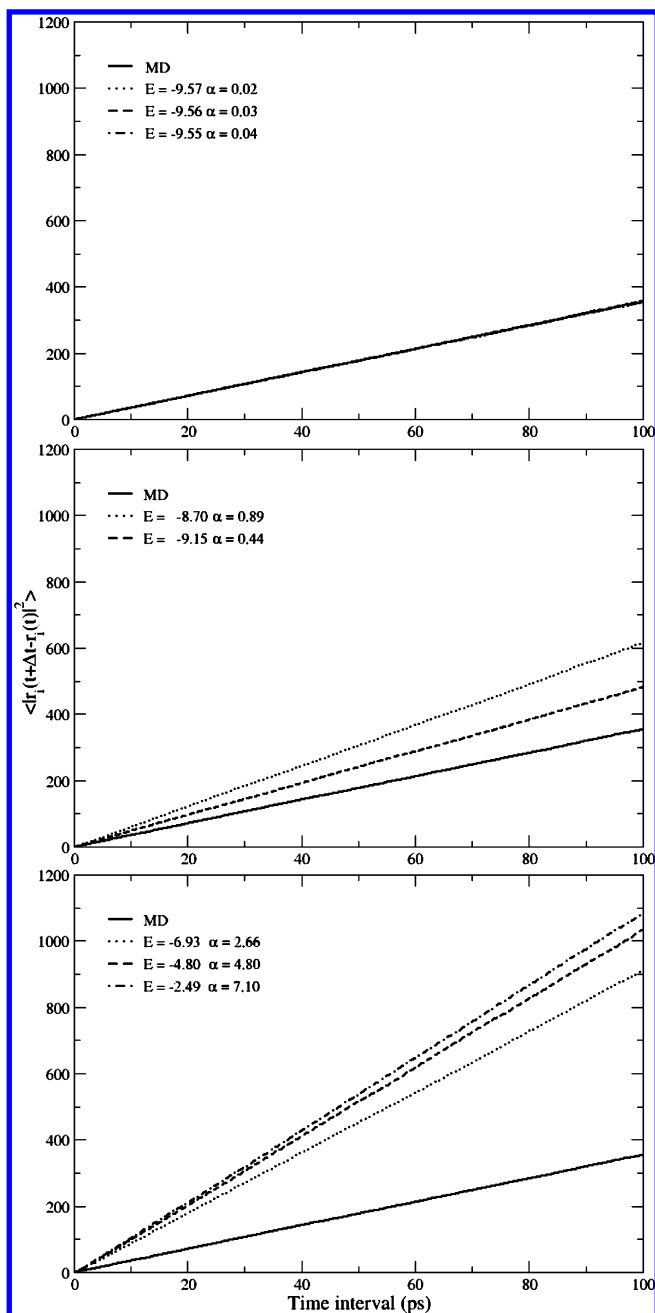


Figure 2. Plots of mean square displacement versus time interval. MD stands for normal molecular dynamics simulation.

correspond to approximately 75%, 50%, and 25% of V_{\min} , we obtained a large increase in the calculated diffusion coefficients. The ratio between the calculated diffusion coefficient for the normal (D_{MD}) and accelerated (D_{ACC}) MD simulations are presented in Table 1. An increase of 2.57-, 2.93-, and 3.07-fold was obtained by setting $E = -6.93$ and $\alpha = 2.66$, $E = -4.80$ and $\alpha = 4.80$, and $E = -2.49$ and $\alpha = 7.10$, respectively. However, these accelerated MD schemes were not able to reproduce, even qualitatively, the oxygen–oxygen radial distribution functions of the normal water simulation. The RDFs in Figure 3c reveal that the water configurations sampled on these modified potentials are clearly less structured than those sampled on the true potential. The R_{oo} values calculated from these accelerated MD trajectories show that while the first peak is broad and underpopulated, the second peak and the trough between the first and second peaks are shifted forward and overpopulated. As a result, the heat of vaporization obtained from

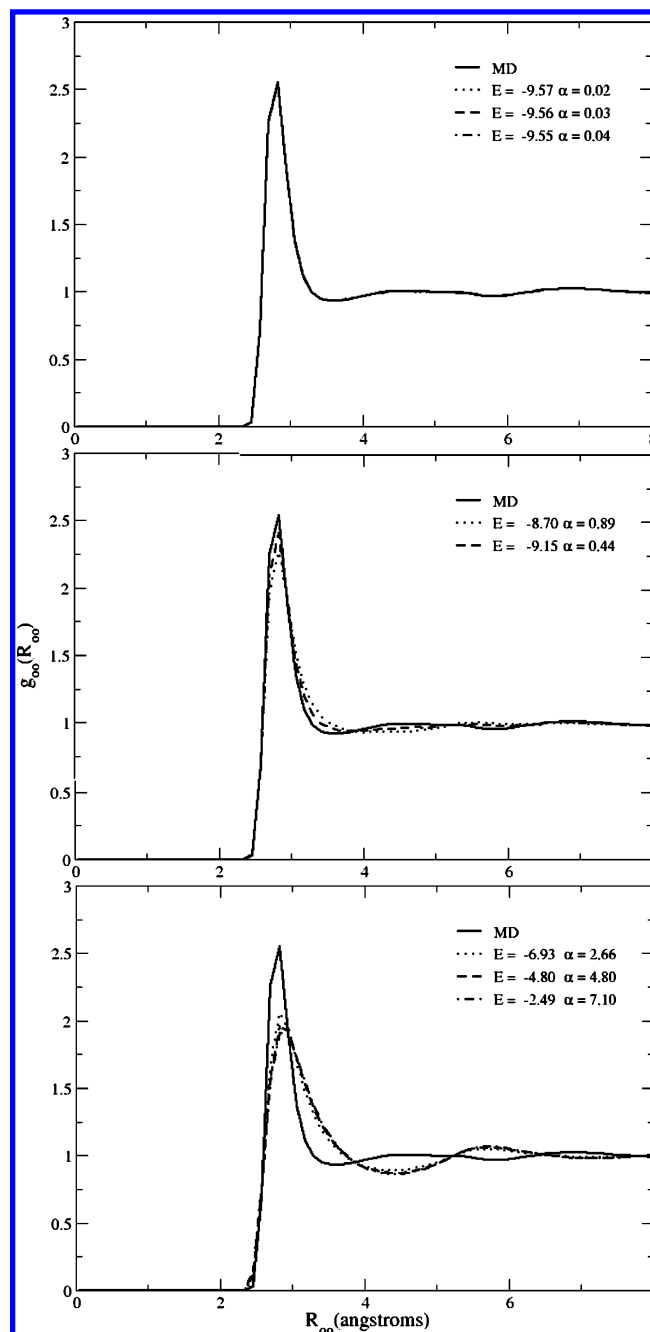


Figure 3. Oxygen–oxygen radial distribution function. MD stands for normal molecular dynamics simulation.

these accelerated MD simulations poorly agrees with the value of 10.13 kcal/mol, calculated from TIP3P water simulations using Ewald summation (Table 1).^{24,25} Figures 2b and 3b show the results of accelerated MD simulations in which we apply $E = -9.15$ and $\alpha = 0.44$ and $E = -8.70$ and $\alpha = 0.89$. Comparing to the normal MD, these accelerated schemes not only increase the calculated diffusion coefficient by 35% and 73%, respectively (Figure 2b), but also clearly improve the ΔH_{vap} (Table 1) and the liquid structure (Figure 3b). The error in heat of vaporization was 0.31 kcal/mol for $E = -9.15$ and $\alpha = 0.44$ and 0.67 kcal/mol for $E = -8.70$ and $\alpha = 0.89$. Although most of the details in the R_{oo} are recovered, its first peak is still lower and broader than the one obtained from normal MD. In addition, the RDFs are nearly flat around the second peak.

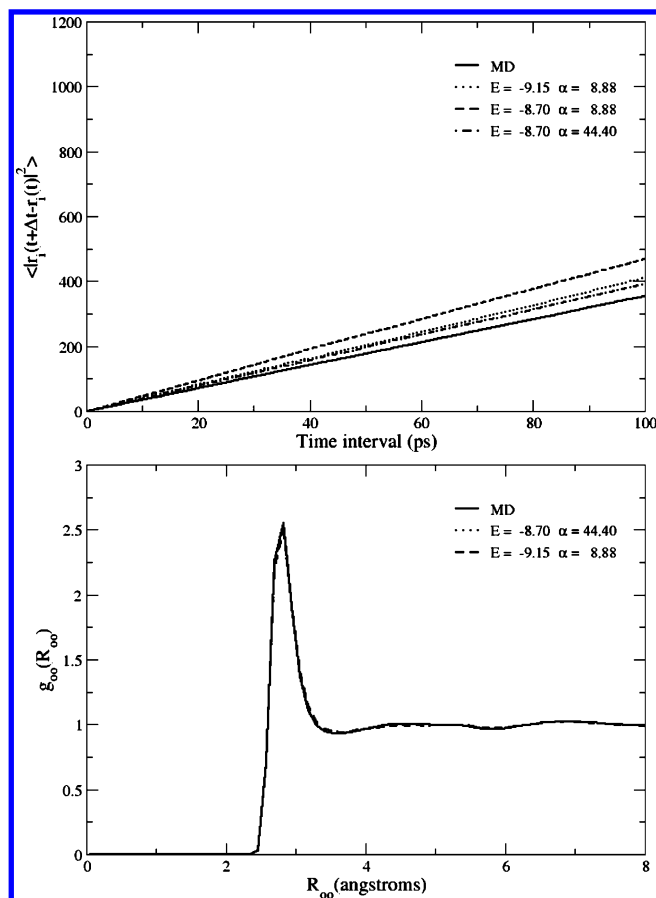


Figure 4. Plots of mean square displacement versus time interval and oxygen–oxygen radial distribution function. MD stands for normal molecular dynamics simulation.

To explore the influence of the parameter α on the water properties, we performed three additional accelerated MD simulations by applying $E = -9.15$ and $\alpha = 8.88$, $E = -8.70$ and $\alpha = 8.88$, and $E = -8.70$ and $\alpha = 44.40$ kcal/mol. As was expected, by setting $E = -9.15$ and $\alpha = 8.88$ and $E = -8.70$ and $\alpha = 44.40$ kcal/mol, we obtained good agreement between the R_{Oo} calculated from the accelerated and normal MD. As was previously described,¹² α is a tuning parameter that controls how deep the energy basins are on the modified potential. Thus, keeping E fixed, the modified potential gradually becomes closer to the true potential as α is increased (Figure 1). In other words, both accelerated and normal MD start sampling configurations from equivalent regions in the phase space. It is clearly observed when we compare the RDFs obtained for $\alpha = 0.89$ (Figure 3b) and 44.40 (Figure 4) kcal/mol, but keeping $E = -8.70$ kcal/mol. As α is increased, the shape and the height of the first and second peaks are improved, as well as the trough between them. It is worth noting that R_{Oo} and ΔH_{vap} have been well reproduced by these accelerated MD schemes, and we still observed increases of 15% and 10% in the diffusion coefficient for these systems (Figure 4, Table 1).

These results show that although the ensemble average on the true potential surface can be recovered by multiplying each configuration by the strength of the bias at each position, in some cases, statistical difficulties make it difficult to sample the true canonical distribution adequately (Figure 3 and Table 1). This is due to poor overlap between the canonical distributions corresponding to the true and the modified potential functions. It is clear that as the strength of the bias potential is increased, the number of truly representative configurations of

liquid water sampled on the modified potential is drastically reduced. In those cases, the only way of increasing the number of configurations which provide useful statistical information is to perform much longer simulations. Otherwise, the poor statistics will prevent recovery of the correct structural and ensemble properties.

Another important property that should be taken into account when we compare different simulation methods is the correlation time, τ . The correlation or relaxation time corresponds to the number of steps required for the system to lose its “memory” of previous configurations. Configurations obtained between steps smaller than τ are so highly correlated to one another that successive steps give little new statistical information. An alternative and efficient procedure for obtaining the correlation time parameter τ is the statistical inefficiency method.^{23,26}

To calculate the statistical inefficiency, s , first, the trajectories are broken down into a series of n_b blocks of size t_b . The average value of the property A (in this work A is the potential energy) for each block is given by

$$\langle A \rangle_b = \frac{1}{t_b} \sum_{i=1}^{t_b} A_i \quad (12)$$

As the number of steps t_b in each block increases, the block averages become increasingly uncorrelated. Besides, the variance of the block averages, $\sigma^2(\langle A \rangle_b)$, become inversely proportional to n_b and is calculated as

$$\sigma^2(\langle A \rangle_b) = \frac{1}{n_b} \sum_{b=1}^{n_b} (\langle A \rangle_b - \langle A \rangle_{\text{total}})^2 \quad (13)$$

where $\langle A \rangle_{\text{total}}$ is the average taken during the entire simulation. The statistical inefficiency, s , is then defined as

$$s = \lim_{t_b \rightarrow \infty} \frac{t_b \sigma^2(\langle A \rangle_b)}{\langle A \rangle_{\text{total}}} \quad (14)$$

For a Markovian process, the correlation time τ relates to the statistical inefficiency as $s \approx 2\tau$. In this work, we consider that configurations obtained after 2τ are uncorrelated. Equation 15 relates s with the error in the average $\langle A \rangle$.

$$\sigma_{\langle A \rangle} \approx \sigma \sqrt{\frac{s}{N_{\text{steps}}}} \quad (15)$$

where $\sigma_{\langle A \rangle}$ and σ are the standard deviation of the average $\langle A \rangle$ obtained from a finite and infinite simulation, respectively. N_{steps} is the number of steps of the finite simulation.

Therefore, it is worth noting that if the accelerated MD method can reduce the statistical inefficiency of the simulation, then more uncorrelated structures are sampled, and as a consequence more accurate average values can be calculated for a given simulation time. To calculate s , we carried out an MD simulation of 440 ps for each system. The potential energy of the system was recorded every time step, but only the last 400 ps were used in the calculation of s . All the simulations were carried out by using the same preequilibrated initial configuration, which corresponds to the last configuration obtained after the equilibration phase performed with the normal MD simulations (see methods and applications). All results are summarized in Table 1.

Figure 5 shows the statistical inefficiency calculated for the normal and accelerated MD trajectories. All accelerated MD

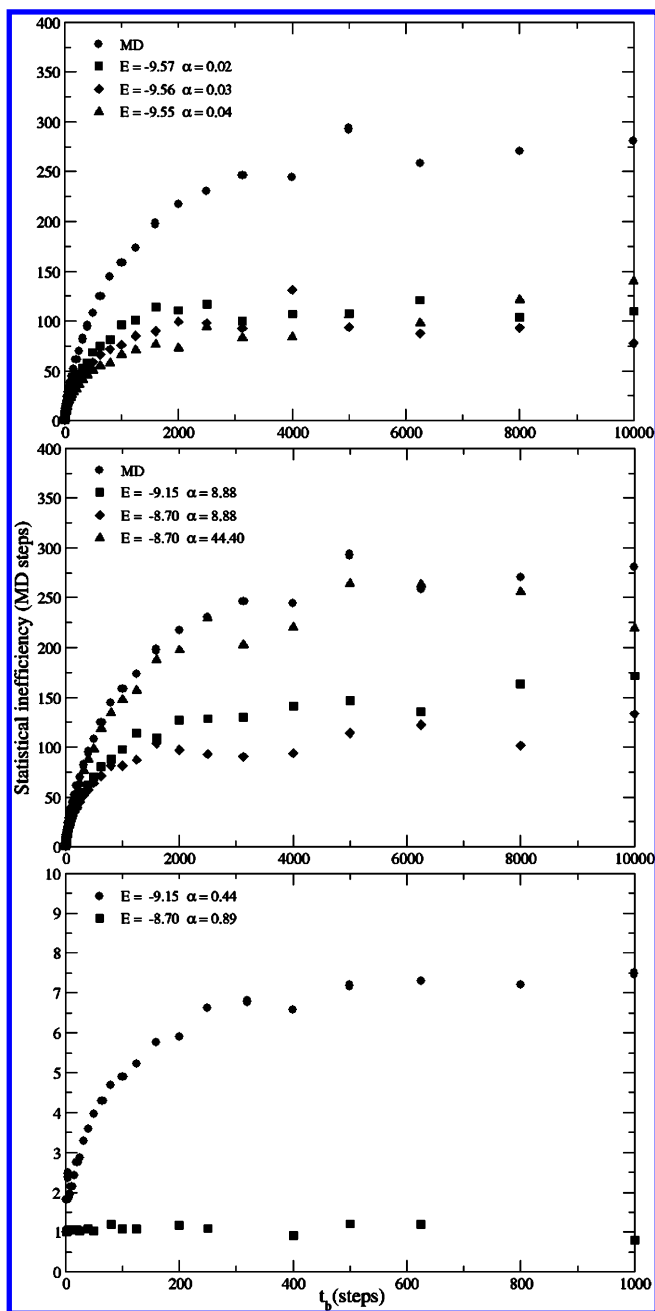


Figure 5. Statistical inefficiency from water simulations. MD stands for normal molecular dynamics simulation.

schemes reduced the correlation time of the simulation, even when low values of boost energy are applied. For those schemes which correspond to $E = -9.57$, -9.56 , and -9.55 kcal/mol, we observed a reduction of at least 2.3-fold in τ . A very interesting result is found when E and α are set to -9.55 and 0.04 kcal/mol, respectively. In this case, not only all the calculated properties, ΔH_{vap} , D and R_{oo} , were very well reproduced but also the correlation time was 4-fold shorter than in the normal MD simulation (Figure 5a). Further reduction in τ is obtained when high values of boost energy are applied. As expected, in the cases where the molecular dynamics is aggressively accelerated, which correspond to $E = -2.49$, -4.80 , and -6.93 kcal/mol, no correlation time was observed, meaning that configurations sampled at each simulation step are uncorrelated to each other. The same result was obtained when E and α were set to -8.70 and 0.89 kcal/mol (Figure 5c). Figure 5b shows the effect of the parameter α over τ . As

was observed for the other properties, the correlation time tends to the value obtained in the normal MD simulation as α is increased. Keeping $E = -9.15$ kcal/mol and increasing α from 0.44 to 8.89 kcal/mol, we observed that the reduction in correlation time changed from 40-fold to 2-fold. Similar results were obtained for $E = -8.70$ kcal/mol when α was increased to 8.88 kcal/mol. While no correlation time was observed when $\alpha = 0.89$, it was increased to approximately half of the value found in the normal MD simulation when $\alpha = 8.88$. It is interesting to note that τ converges to the value calculated in the normal MD when α is further increased to 44.40 kcal/mol (Figure 5b).

Conclusion

The results presented in this work show that this new simulation technique can accelerate the molecular motions of liquid water without losing its microscopic structure and equilibrium properties. We show that the application of a small boost energy E on the potential-energy surface significantly reduces the statistical inefficiency of the simulation while keeping all the other calculated properties unchanged. For instance, when E and α were set to -9.55 and 0.04 kcal/mol, respectively, we observed that the correlation time calculated with the modified potential was 4-fold lower than the one obtained in the normal MD simulation. As a consequence, this modified energy landscape allows the liquid water to equilibrate approximately four times faster. This result suggests that, although the application of small boost energy is able to significantly accelerate the configurational changes of water molecules, increasing $\tau_{\text{MD}}/\tau_{\text{ACC}}$, these configurational changes may not be frequent enough to increase the self-diffusion coefficient of water molecules. Other interesting results were obtained with $E = -9.15$ and $\alpha = 8.88$ kcal/mol. In this case, we not only reduced the statistical inefficiency of the water simulation, but also increased the diffusion of water molecules by 15%. One of the potential applications of these schemes lies in the free energy perturbation calculations (ongoing investigations). Since this method enhances configurational sampling and allows a faster relaxation of water molecules as compared to normal MD, it may significantly improve the convergence and accuracy of free energy calculations with explicit solvent.

It is interesting to mention that, setting $E = -9.15$ and $\alpha = 0.44$ kcal/mol, it was possible to increase significantly the mobility of water molecules (35%) while the main structural features of the liquid water were reasonably preserved. Moreover, the correlation time calculated in this scheme was 40-fold lower than in normal MD. Since this case provided a good balance between high acceleration of molecular motions and recovery of the ensemble average properties, it would be of great value in the study of long time scale conformational changes of biomolecules by using all-atom simulations with explicit description of the solvent.

Our results showed that aggressive acceleration of the dynamic simulation results in deleterious effects on the radial distribution function and ΔH_{vap} . Although the application of high boost energy increases the self-diffusion coefficient of water molecules greatly and dramatically reduces the correlation time of the simulation, configurations representative of the true structure of liquid water are poorly sampled. The results also suggest that, in those conditions, the modified potential surface becomes relatively flat over large parts of configuration space. In this case, most part of the phase space regions visited by the accelerated MD simulation may correspond to regions of relatively high energy in the true potential-energy surface. As

a consequence, the truly representative configurations of liquid water are visited rarely on this modified landscape. Thus, although aggressive acceleration conditions enhance dramatically the conformational sampling in water simulations, much longer simulation may be required to recover the truly structural and ensemble average properties. To obtain additional gains in sampling efficiency, one very interesting approach is to combine the accelerated MD with other methods that speed sampling by using other approaches than those that modify the potential surface, e.g., by altering the masses of the lightest atoms.²⁷ Therefore, we should keep in mind that there is a compromise between the strength of the boost applied in the simulation and the reproduction of the ensemble average properties.

Acknowledgment. This work was supported in part by grants from NSF, NIH, the Center for Theoretical Biological Physics, the National Biomedical Computation Resource, San Diego Supercomputing Center, and Accelrys, Inc.

References and Notes

- (1) Guillot, B. *J. Mol. Liq.* **2002**, *101* (1–3), 219–260.
- (2) Israelachvili, J.; Wennerstrom, H. *Nature (London)* **1996**, *379*, 219–225.
- (3) Bashford, D.; Case, D. *Annu. Rev. Phys. Chem.* **2000**, *51*, 129–152.
- (4) Roux, B.; Simonson, T. *Biophys. Chem.* **1999**, *78*, 1–20.
- (5) Schafer, H.; Daura, X.; Mark, A. E.; van Gunsteren, W. F. *Proteins* **2001**, *43*, 45–56.
- (6) Karim, O.; McCammon, J. A. *J. Am. Chem. Soc.* **1986**, *108*, 1762–1766.
- (7) Guimaraes, C. R. W.; Barreiro, G.; de Oliveira, C. A. F.; Alencastro, R. B. *Braz. J. Phys.* **2004**, *34*, 126–136.
- (8) Zhou, R.; Berne, B. J. *Proc. Natl. Acad. Sci. U.S.A.* **2002**, *99*, 12777–12782.
- (9) Daura, X.; Mark, A. E.; van Gunsteren, W. F. *Comput. Phys. Commun.* **1999**, *123*, 97–102.
- (10) Hamelberg, D.; McCammon, J. A. *J. Am. Chem. Soc.* **2004**, *126*, 7683–7689.
- (11) Liang, Po-H.; Brun, K. A.; Feild, J. A.; O'Donnell, K.; Doyle, M. L.; Green, S. M.; Baker, A. E.; Blackburn, M. N.; Abdel-Meguid, S. S. *Biochemistry* **1998**, *37*, 5923–5929.
- (12) Hamelberg, D.; Mongan, J.; McCammon, J. A. *J. Chem. Phys.* **2004**, *120*, 11919–11929.
- (13) Voter, A. F. *Phys. Rev. Lett.* **1997**, *78*, 3908–3911.
- (14) Voter, A. F. *J. Chem. Phys.* **1997**, *106*, 4665–4677.
- (15) Hamelberg, D.; Shen, T.; McCammon, J. A. *J. Am. Chem. Soc.* **2005**, *127*, 1969–1974.
- (16) Cukier, R. I.; Morillo, M. J. *J. Chem. Phys.* **2005**, *123*, 234908.
- (17) Jorgensen, W. L.; Chandrasekhar, J.; Madura, J. D.; Impey, R. W.; Klein, M. L. *J. Chem. Phys.* **1983**, *79*, 926–935.
- (18) Case, D. A.; Perlman, D. A.; Caldwell, J. W.; Chetham, T. E., III; Ross, W. S.; Simmerling, C. L.; Darden, T. A.; Merz, K. M.; Stanton, R. V.; Cheng, A. L.; Vincent, J. J.; Crowley, M.; Tsui, V.; Gohlke, H.; Radmer, R. J.; Duan, Y.; Pitera, J.; Massova, I.; Seibel, G. L.; Singh, U. C.; Weiner, P. K.; Kollman, P. A. *AMBER7*, University of California: San Francisco, CA, 1995.
- (19) Hockney, R. W. *Methods Comput. Phys.* **1970**, *9*, 136–211.
- (20) Berendsen, H. C. J.; Postma, J. P. M.; van Gunsteren, W. F.; DiNola, A.; Haak, J. R. *J. Chem. Phys.* **1984**, *81*, 3684–3690.
- (21) Essmann, U.; Perera, L.; Berkowitz, M. L.; Darden, T.; Lee, H.; Pedersen, L. G. *J. Chem. Phys.* **1995**, *103*, 8577–8593.
- (22) Ding, H. Q.; Karasawa, N.; Goddard, W. A. *J. Chem. Phys.* **1992**, *97*, 4309–4315.
- (23) Allen, M. P.; Tildesley, D. J. In *Computer Simulation of Liquids*; Clarendon: Oxford, U.K., 1987.
- (24) Price, D. J.; Brooks, C. L. *J. Chem. Phys.* **2004**, *121*, 10096–10103.
- (25) Mark, P.; Nilsson, L. *J. Comput. Chem.* **2002**, *23*, 1211–1219.
- (26) Cautinho, K.; Canuto, S. *Adv. Quantum Chem.* **1997**, *28*, 89–98.
- (27) Pomes, R.; McCammon, J. A. *Chem. Phys. Lett.* **1990**, *166*, 425–428.